



HAL
open science

Effect of a zinc oxide, at the cathode interface, on the efficiency of inverted organic photovoltaic cells based on the CuPc/C(60) couple

Y. Lare, M. Banéto, Linda Cattin, M. Morsli, K. Jondo, K. Napo, J. Bernède

► To cite this version:

Y. Lare, M. Banéto, Linda Cattin, M. Morsli, K. Jondo, et al.. Effect of a zinc oxide, at the cathode interface, on the efficiency of inverted organic photovoltaic cells based on the CuPc/C(60) couple. *Journal of Materials Science: Materials in Electronics*, 2011, 22 (4), pp.365-370. 10.1007/s10854-010-0143-6 . hal-00849468

HAL Id: hal-00849468

<https://hal.science/hal-00849468>

Submitted on 30 Oct 2023

HAL is a multi-disciplinary open access archive for the deposit and dissemination of scientific research documents, whether they are published or not. The documents may come from teaching and research institutions in France or abroad, or from public or private research centers.

L'archive ouverte pluridisciplinaire **HAL**, est destinée au dépôt et à la diffusion de documents scientifiques de niveau recherche, publiés ou non, émanant des établissements d'enseignement et de recherche français ou étrangers, des laboratoires publics ou privés.

Effect of a zinc oxide, at the cathode interface, on the efficiency of inverted organic photovoltaic cells based on the CuPc/C₆₀ couple

Y. Lare, M. Banéto, L. Cattin, M. Morsli, K. Jondo, K. Napo, J. C. Bernède

Abstract The effect of ZnO buffer layer on the performances of inverted multilayers organic solar cells has been studied. ZnO:Al conductive films and insulating ZnO films deposited by spin coating have been probed. The ZnO buffer layer has been introduced between the ITO cathode and the Organic acceptor. The cells are based on the multilayer junctions bathocuproine/fullerene/copper phthalocyanine. The organic photovoltaic cells performances improvement depends of the ZnO layer introduced. ZnO:Al conductive layers decreases the potential barrier at the interface cathode/organic. This allows decreasing the series resistance which improves significantly the cell efficiency. Insulating ZnO increases only slightly the solar cells performance by increasing significantly the shunt resistance and therefore the open circuit voltage of the cells.

1 Introduction

The active heart of organic photovoltaic cells (OPV cells) consists either of two organic layers or an homogeneous mixture of two organic materials [1, 2]. One of them, either an organic dye or a semi conducting polymer, donates the

electrons. The other serves as electron acceptor. OPV cells with power conversion efficiency (PCE) of 5–6% under simulated AM1.5 illumination have been obtained [3–5]. Usually, in these devices, an indium tin oxide, (ITO), coated glass substrate is used as transparent anode and an aluminium thin film as cathode. The classical multi-heterojunction structures are based on ITO/anode buffer layer/CuPc/C₆₀/cathode buffer layer/Al devices where CuPc is the copper phthalocyanine and C₆₀ the fullerene. The buffer layers (BF) are necessary in view of the difficulties in organic optoelectronic devices of the charge carrier transport between the organic materials and the electrodes. In the case of the anode/electron donor contact, a common solution is to introduce a thin anode buffer layer (ABL), which adjusts the electronic behaviour of the adjacent materials. We have shown that an ultra-thin metal film or a thin oxide film deposited onto the conductive substrate, whatever the transparent conductive oxide (TCO), can be used to improve the interface TCO/donor and therefore the devices performances [6–8].

It has been shown that, when a large band gap material, such as bathocuproine (BCP) [9] or aluminium tris(8-hydroxyquinoline) (Alq₃) [10, 11], is introduced between the cathode and the electron acceptor, there is a strong improvement of the OPV cells performances. This layer is called exciton blocking layer (EBL). It should be transparent to the solar spectrum to act as a spacer between the photoactive region and the metallic cathode. It must, also, transport electrons to avoid high series resistance.

If the classical devices described above have given the best performances, development of inverted solar cells could allow more flexibility on designing tandem structures, which can be formed using a semitransparent cathode. In an inverted device the TCO is the cathode and the metal electrode is the anode. Up to now, the inverted

Y. Lare · M. Banéto · K. Jondo · K. Napo
CUER-UL, Université de Lomé, Lomé, Togo

L. Cattin
Université de Nantes, Institut des Matériaux Jean Rouxel (IMN),
CNRS, 2 rue de la Houssinière, BP 32229, 44322 Nantes
cedex 3, France

M. Morsli · J. C. Bernède (✉)
Université de Nantes, Nantes Atlantique Universités,
LAMP, EA 3825, Faculté des Sciences et des Techniques,
2 rue de la Houssinière, BP 92208, 44000 Nantes, France
e-mail: jean-christian.bernede@univ-nantes.fr

organic solar cells studied are usually based on bulk heterojunctions and promising results have been obtained [12–14], while no many works have been dedicated to inverted multi-heterojunction PV cells [15]. The challenge to reversing the layer sequence of multi-heterojunction PV cells is achieving cathode and anode ohmic contacts. We have already shown that the presence of a thin BCP layer at the interface ITO cathode/ C_{60} allows improving OPV cells performances in the same way that in classical ones [16]. In the present work we study the effect of a zinc oxide buffer layer, at the cathode interface, on the efficiency of inverted OPV cells based on the BCP/CuPc/ C_{60} multi-heterojunction structure.

2 Experimental

The device structure used in this study is:

ITO/CBL/BCP(9nm)/ C_{60} (40nm)/CuPc(35nm)/ABL/Al

Here CBL is a buffer layer which allows achieving a good matching between the ITO cathode and the organic material. The multi-layer heterojunction structure used in the present work has ITO/CBL as bottom cathode and ABL/Al as anode. The buffer layer ABL is used to achieve a good matching between the work function of the anode and the highest occupied molecular orbital (HOMO) of CuPc. We have already shown that Au, MoO_3 [6, 7] or, better, MoO_3/Au , allows achieving this goal [8], by simple vacuum deposition of a thin (3.5 ± 1 nm) MoO_3 film, of an ultrathin (0.5 nm) gold film or of MoO_3/Au superposed films. The best results were achieved with this last combination. Therefore, we used MoO_3/Au as ABL buffer layer.

The effect of the CBL on the properties of the inverted organic solar cell is the subject of this work. Here, CBL is a conductive or insulating ZnO film. Therefore, the structures probed were:

ITO/ZnO/BCP(9 nm)/ C_{60} (40 nm)/CuPc(35 nm)/
ABL/Al,

the ZnO being conductive (ZnO:Al) or insulating (ZnOsc).

The ITO coated glass substrates used in this study were commercially obtained from the SOLEMS. Since ITO covered the whole glass substrates, some ITO must be removed to obtain the bottom electrode. After masking a broad band of 30 mm by 20 mm, the ITO was etched by using Zn + HCl. After carefully scrubbing, with alcohol and then soap, these substrates were rinsed in running deionised water. The substrates were dried and immediately loaded into a vacuum chamber (10^{-4} Pa) when the ZnO films were obtained by rf magnetron sputtering

(ZnO:Al) or introduced into a hood, when they were deposited by spin coating (ZnOsc).

The chemical products (CuPc, C_{60} , BCP...Au, MoO_3) have been provided by Aldrich. All the thin films of the structures have been deposited in the same run in a vacuum of 10^{-4} Pa. The thin film deposition rates and thickness were estimated in situ with a quartz monitor. The deposition rate and final thickness were 0.1 nm/s and 9 nm for BCP, 0.05 nm/s and 35 nm in the case of CuPc and 0.05 nm/s and 40 nm in the case of C_{60} . These thicknesses have been chosen after optimisation.

In the case of the buffer layer ABL, the known optimum thickness have been used, 3 nm for MoO_3 [8] and 0.5 nm for Au [6, 7]. For the CBL, the ZnO thickness probed were 0, 3 and 5 nm.

After ABL (MoO_3/Au) deposition, the aluminium top electrode was thermally evaporated, without breaking the vacuum, through a mask with 2×8 mm active areas, and following by 50 nm thick encapsulating layer of amorphous selenium (Se-a). The selenium protective coating layer has been proved to be efficient to protect the under layers from oxygen to water vapour contamination [17], at least during the first hours of room air exposure [11].

The conductive ZnO films were deposited by ac magnetron sputtering on glass substrates at room temperature. A cylindrical target of diameter 75 mm and thick of 5 mm was prepared by sintering the mixture of ZnO powder (purity of 99.99%) with 2wt% Al_2O_3 (purity 99.99%). Ar (99.99%), source is used as sputtering gas for deposition of the ZnO:Al films. The distance between target and substrate was about 60 mm. The flow rate of Argon was controlled by using flow meter. The sputtering pressure was maintained at 0.13 Pa. The pressure of the sputtering system before the deposition of the sample films was under 2×10^{-3} Pa. The films were deposited onto substrates under 150 W. These deposition conditions were fixed in order to achieve ZnO:Al conductive transparent films. The conductivity of the obtained films has been checked, using a ZnO:Al film thick of 100 nm, it is around $\sigma = 2.32 \times 10^3$ (Ω cm) $^{-1}$.

The insulating films were deposited by spin coating. Appropriate amount of zinc nitrate (0.05 mol/l) and ammoniac (0.1 mol/l) were mixed. The pH of the bath was 8.0. The solution was maintained at a temperature $60^\circ C < T < 65^\circ C$, while the bath was continuously stirred. 0.5 ml of this solution was deposited by spin coating onto ITO glass coated substrate, the spin speed was 2,000 rpm and the spin time was 60 s. The coated films were then annealed at 300 K for 1 h in order to change the $Zn(OH)_2$ into ZnO polycrystalline films. The thickness of the ZnO films was estimated using an atomic force microscope apparatus (AFM).

The ZnO films have been characterized by different techniques. The morphology was observed through scanning electron microscopy (SEM) with a JEOL 6400F at the “Centre de Microcaractérisation de l’Université de Nantes”. The crystalline structure of the films was analyzed by X-ray diffraction (XRD) by a Siemens D 5000 diffractometer using $K\alpha$ radiation from Cu ($\lambda = 0.15406$ nm). AFM images on different sites of the film were taken ex-situ at atmospheric pressure and room temperature. All measurements have been performed in tapping mode (Nanoscope III, (Digital Instruments, Inc.). Classical SiN4 cantilevers were used (Ultrasharp, AXESSTECH, France). The average force constant and resonance were approximately 14 N/m and 320 kHz, respectively. The cantilever was excited at its resonance frequency.

Electrical characterizations were performed with an automated I–V tester, in the dark and under one sun global AM 1.5 simulated solar illumination. Performances of photovoltaic cells were measured using a calibrated solar simulator (Oriel 300 W) at 100 mW/cm^2 light intensity adjusted with a PV reference cell (0.5 cm^2 CIGS solar cell, calibrated at NREL, USA). Measurements were performed at an ambient atmosphere. All devices were illuminated through TCO electrodes.

3 Experimental results

XRD and microprobe analysis have been measured on 100 nm ZnO thick films, while the OPV cells have been achieved with 3–7 nm thick films.

XRD patterns (not shown here) of ZnO:Al films show that they crystallize in the hexagonal system with a wurtzite structure. Their crystallites are preferentially oriented along the c-axis (002) perpendicular to the substrate surface [18]. The spin coated ZnO films (ZnO_{SC}) are also crystallized in the hexagonal wurtzite structure; however, their crystallites are randomly oriented.

The measurements of films composition have been done by EPMA analysis. This technique allows estimating oxygen atomic concentration, however, the precision of the measure decreases with the atomic weight of the element, therefore, the results show that the films, whatever the deposition technique used, are nearly stoichiometric with a slight oxygen deficiency (1–3 at.%). For ZnO:Al films 2 at.% of Al is measured.

The surface morphology of the ZnO thin films has been studied by SEM and AFM. The SEM study shows that the surface of the sputtered ZnO:Al is smooth (Fig. 1a), while that of ZnO_{SC} films is inhomogeneous (Fig. 1b). A high density of clusters randomly distributed on the film surface is clearly visible. However, the layer itself appears quite smooth. These films have been submitted to the scotch tape

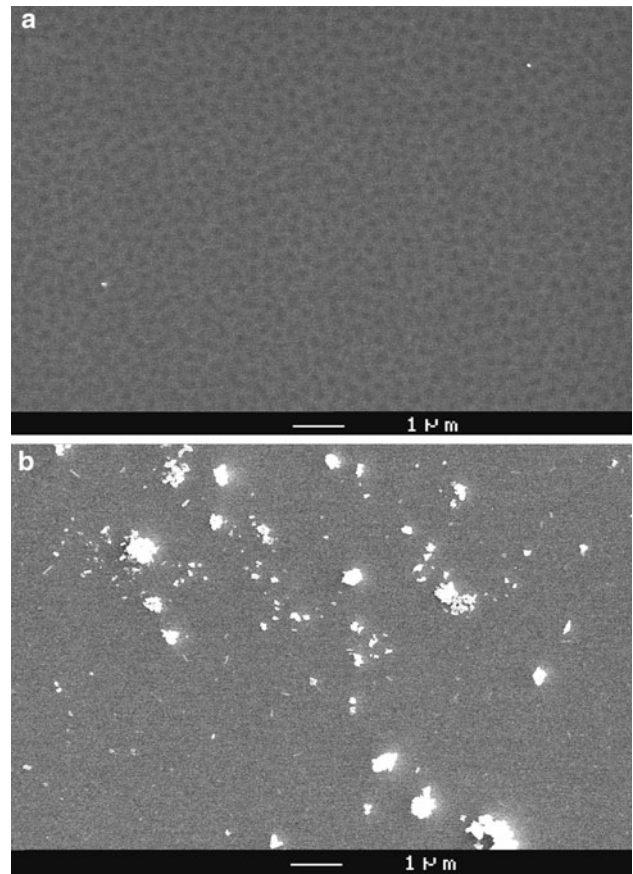


Fig. 1 Surface visualization of a ZnO:Al (a) and a ZnO_{sc} film (b)

test. Such test is usually used to measure the adhesion of a deposited film to the substrate. Here it is used to clean the deposited film since the ZnO clusters at the surface of the films are not good adhesion to the homogeneous layer of ZnO. It is known that precipitation can take place either in the bulk of the solution with the formation of colloids by an homogeneous reaction or at the surface of the substrates leading to the formation of an homogeneous film by an heterogeneous reaction. A predominantly homogeneous reaction often terminates the heterogeneous, and the film grows by absorption of colloids, leading to superficial heterogeneities. Therefore, the compact layer, which corresponds to the heterogeneous reaction, is covered during the growth process by colloids formed by the homogeneous reaction in the solution bulk (Fig. 1b).

The visualization, in Fig. 2 of the surface of a ZnO_{SC} film, in which half surface (right side) has been submitted to this test, shows that the clusters have been removed by the scotch tape. It allows seeing that the surface of the film itself is smooth and homogeneous. These surfaces, before and after the scotch tape cleaning, have been checked by AFM study. Before cleaning, large “maximum roughness peaks”, out of scale, are present. After cleaning, one can see in Fig. 3 that the ZnO_{SC} buffer layers are quite

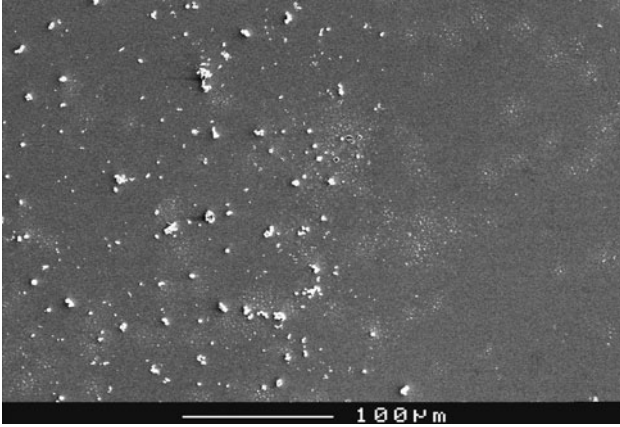


Fig. 2 Surface visualization of a ZnO film deposited by spin coating: *left side* before scotch test and *right side*, after the scotch test

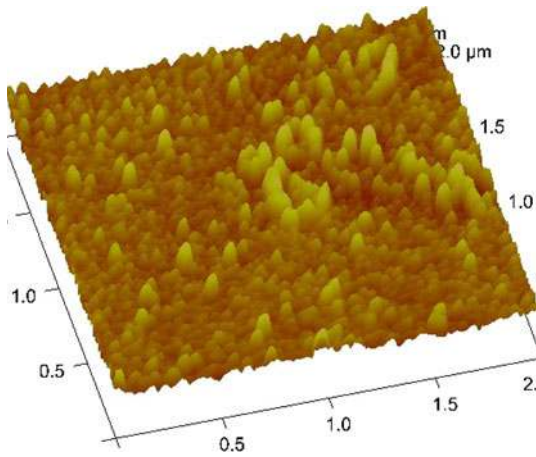


Fig. 3 TM-AFM images of thin films of FTO_{SP} after scotch tape cleaning

homogeneous with a Root Means Square (RMS) surface roughness of 1 nm. The averaged thickness estimated from AFM is around 4 nm.

The conductivity of the ZnO:Al films is around $\sigma = 2.32 \times 10^3 (\Omega \text{ cm})^{-1}$. As expected the ZnOsc films are insulating, with σ less than $10^{-5} (\Omega \text{ cm})^{-1}$. These values have been measured on 100 nm thick film.

After characterization the different ZnO thin films have been used as buffer layer in the inverted organic solar cells ITO/ZnO/BCP/C₆₀/CuPc/MoO₃/Au/Al.

In a first time, we have optimized the ZnO thickness using ZnO:Al films. The ZnO:Al film thickness was 0, 3

and 5 nm. The results are summarized in Table 1. It can be seen that the optimum ZnO:Al thickness is 3 nm. For thicker or thinner ZnO films all the characteristics are degraded. The short circuit current and open circuit voltage decreases significantly.

In the case of ZnO_{SC}, the results depend strongly on the morphology of the anode surface. Following the AFM results, the mean thickness of the films used, was around 4 nm. When the ZnO_{SC} cleaned film is used as buffer layer, the J-V characteristics exhibit diode rectifying effect, while they do not, when it is not cleaned. For such inhomogeneous films, the rectifying effect is destroyed. The clusters, as visible in Fig. 1b, have mean diameter far higher than the whole thickness of the organic active films and therefore they induce strong inhomogeneity in the growth of the organic film with short path, pinholes..., which results in high density of defaults in the organic thin films and small shunt resistance. As a consequence, the J-V characteristics are more or less ohmics.

After cleaning, the film surface is homogeneous and a photovoltaic effect is obtained. Table 2 and Fig. 4 summarize the effect of the nature of the ZnO film on the solar cells performances, it can be seen that the best results are achieved using the conductive ZnO:Al buffer layer. It should be noted that the highest Voc value is obtained with ZnOsc. The ZnOsc being nearly insulating it increases the shunt resistance and therefore the Voc value. However, the high resistivity of the ZnOsc induces also smaller short circuit current and finally smaller efficiency that that obtained with conductive ZnO:Al. From these results, if we exclude the rough ZnO_{SC}, it can be said that the presence of a smooth ZnO film, conductor or not, improves the cells performances even if the best results are achieved with the conducting ZnO:Al.

4 Discussion

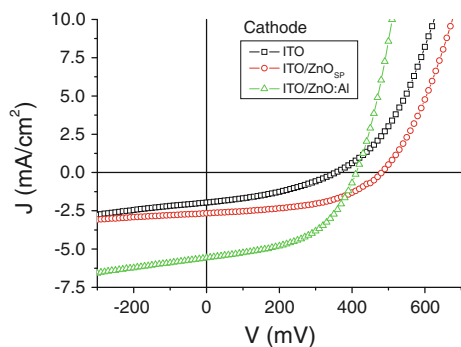
First of all, for classical multilayer heterojunction OPV cells, it is known that one way for circumventing the diffusion length limitation of the excitons is to use cells with multiple interfaces. Peumans et al. [9] have shown that the introduction of a thin large band gap organic material allows improving significantly the device performances. He called electron blocking layer (EBL) this thin film,

Table 1 Effect of the ZnO:Al thickness on the solar cells performances

OPV structure	Jsc (mA/cm ²)	Voc (V)	FF (%)	η (%)
ITO/BCP/C ₆₀ /CuPc/MoO ₃ /Au/Al	3.50	0.355	36.1	0.44
ITO/ZnO:Al(3 nm)/BCP/C ₆₀ /CuPc/MoO ₃ /Au/Al	6.73	0.415	39.7	1.11
ITO/ZnO:Al(5 nm)/BCP/C ₆₀ /CuPc/MoO ₃ /Au/Al	3.11	0.335	38.3	0.40

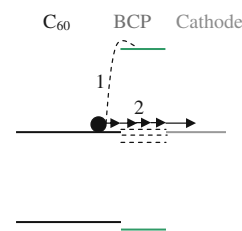
Table 2 Performances of solar cells using different ZnO CBL layers

OPV structure	Jsc (mA/cm ²)	Voc (V)	FF (%)	η (%)	Rs(Ω)	Rsh(Ω)
ITO/BCP/C ₆₀ /CuPc/MoO ₃ /Au/Al	3.55	0.350	35	0.40	787	4,096
ITO/ZnO _{SC} /BCP/C ₆₀ /CuPc/MoO ₃ /Au/Al	2.67	0.485	38.2	0.49	375	7,325
ITO/ZnO:Al/BCP/C ₆₀ /CuPc/MoO ₃ /Au/Al	7.46	0.415	49.7	1.54	156	3,125

**Fig. 4** J-V characteristics of organic solar cells using different cathode buffer layers between the ITO cathode and the C₆₀ electron acceptor

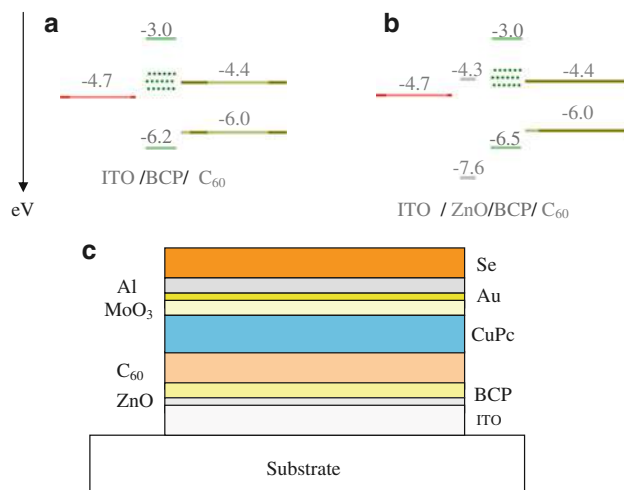
because its band gap is substantially larger than those of the organic donor and acceptor, which blocks excitons in the organic semiconducting layer far from the cathode avoiding any quenching effect at the interface cathode/organic. The EBL confines the photogenerated excitons to the domain near the interface where the dissociation takes place and prevents parasitic exciton quenching at the photosensitive organic/electrode interface. Also it limits the volume over which excitons may diffuse. For these reasons we have introduced a BCP EBL at the interface ITO/electrode acceptor in our inverted OPV cells [16]. This EBL should be transparent to the solar spectrum to act as a spacer between the photoactive region and the metallic cathode. It must, also, transport electrons to avoid high series resistance. If the EBL block the excitons, it should not block all charge carriers. Therefore, the EBL should be chosen so that it allows electrons collection at the cathode. However, the optimum EBL thickness is 8–9 nm, which is too thick to allow high tunnelling current. So it has been suggested that the charge transport in the EBL is due to damage induced during deposition of the upper layers, which introduces conducting levels below its LUMO and explains the reason why the transport of electron is not weakened. [19] (Fig. 5). Therefore, since it is admitted that the EBL is transparent to electron, in a first approach, we will discuss the behaviour of the contact with the cathode as a simple contact ITO/ZnO/organic electron acceptor.

We have shown in a preceding paper [20] that, even if some dipole effect is often present at the interface due to interface states, in a first approach, the behaviour of the

Fig. 5 Band schemes of organic films and cathode contact, with schematized conducting levels below the BCP LUMO

contact electrode/organic material can be roughly anticipated using the Schottky–Mott model. Therefore, the different band scheme configurations of the interface anode/CBL/C₆₀, are presented in Fig. 6. The excitons are generated from irradiated CuPc, then they are dissociated by Coulomb attraction to electrons and holes at the interface CuPc/C₆₀. The holes may be transported directly to the anode through the ABL, which improves the hole collection efficiency [6–8]. At the same time, a good band matching between the cathode work function and the electron acceptor for achieving ohmic contact and good electron collection is necessary.

The treatment of the ITO surface usually has strong influence on the performances of the ITO devices. For example, O₂ plasma treatment increases the work function of ITO, thus enhancing the hole collection in classical organic solar cells. In the present work we have only removed its surface contaminants. However, the work

**Fig. 6** a, b Band scheme of the different contacts ITO/CBL/C₆₀ c Typical OPV cell structure

function of cleaned ITO is still too high, around 4.7 eV, the LUMO of C₆₀ being 4.4 eV, an energy barrier exists for the electron collection from C₆₀ to ITO cathode (Fig. 6a). The collection barrier for electrons from C₆₀ to ITO corresponds roughly [17] to the energy difference between the work function of ITO and the LUMO of C₆₀. The work function of ZnO:Al being 4.3 eV, the electron collection barrier decreased from 0.3 eV for cleaned ITO to nearly 0 for ZnO:Al capped cathode (Fig. 6b). Therefore, the interfacial layer plays an important role in lowering the potential barrier between ITO and C₆₀ and consequently it should increase the collected electron current and the solar cells efficiency. The significant decrease of the potential barrier between ITO and C₆₀ is confirmed by the large decrease of the series resistance (Table 2). This ZnO positive effect is obtained only if ZnO is degenerated, which is the case of ZnO:Al, in the case of the insulating ZnOsc the behaviour of the contact is different. Effectively, if we introduce an insulating film, (I), between the degenerated semiconductor (ITO), and the semiconductor, (S), the contact behaves like a MIS structure. It means that there is not band alignment between the TCO, the insulating layer and the organic semiconductor. However, an electric field appears on the insulating layer, which contributes to some decrease of the potential barrier [8]. This results from the fact that the Fermi level must be constant throughout the metal/insulating layer/semi-conductor. Here also it can be seen Table 2 that there is some decrease of the series resistance. However, the most significant information in Table 2 for ZnOsc is the strong increase in the shunt resistance which justifies the high Voc value.

5 Conclusion

As a conclusion, the improved inverted OPV cells performances can be ascribed to the inserted ZnO interfacial layer. When a conductive ZnO:Al buffer layer is introduced between the ITO cathode and the organic layer it allows a good band matching between the cathode and the LUMO of the organic material, which decreases the potential barrier at the interface cathode/organic material. Such effect is corroborated by the large decrease of the series resistance of these OPV cells. When an insulating

ZnOsc is used as buffer layer, its high resistivity increases significantly the shunt resistance of the OPV cells, which increases significantly the open circuit voltage of the OPV cells.

Acknowledgments This work has been financially supported by the AUF Convention PCSI 6313PS839.

References

1. J.C. Bernède, A. Godoy, L. Cattin, F.R. Diaz, M. Morsli, M.A. del Valle, in *Organic Solar Cells Performances Improvement Induced by Interface Buffer Layers*, ed. R.D. Rugesu, (Solar Energy, 2010) p. 223
2. W. Cai, X. Gong, Y. Cao, *Sol. Energy Mater. Sol. Cells* **94**, 114 (2010)
3. Y. Liang, Z. Xu, J. Xia, S.-T. Tsai, Y. Wu, G. Li, C. Ray, L. Yu, *Adv. Mater.* **22**, 1 (2010)
4. J.Y. Kim, K. Lee, N.E. Coates, D. Moses, T.Q. Nguyen, M. Dante, A.J. Heeger, *Science* **317**, 222 (2007)
5. J. Xue, B.P. Rand, S. Uchida, S.R. Forrest, *J. Appl. Phys.* **98**, 124903 (2005)
6. J.C. Bernède, Y. Berredjem, L. Cattin, M. Morsli, *Appl. Phys. Lett.* **92**, 083304 (2008)
7. J.C. Bernède, L. Cattin, M. Morsli, Y. Berredjem, *Sol. Energy Mater. Sol. Cells* **92**, 1508 (2008)
8. L. Cattin, F. Dahou, Y. Lare, M. Morsli, R. Tricot, K. Jondo, A. Khelil, K. Napo, J.C. Bernède, *J. Appl. Phys.* **105**, 034507 (2009)
9. P. Peumans, V. Bulovic, S.R. Forrest, *Appl. Phys. Lett.* **79**, 2650 (2000)
10. Q.L. Song, F.Y. Li, H. Yang, H.R. Wu, X.Z. Wang, W. Zhou, J.M. Zhao, X.M. Ding, C.H. Huang, X.Y. Hou, *Chem. Phys. Lett.* **416**, 42 (2005)
11. Y. Berredjem, N. Karst, A. Boulmouk, A.H. Gheid, A. Drici, J.C. Bernède, *Eur. Phys. J. Appl. Phys.* **40**, 163 (2007)
12. J. Meiss, N. Allinger, M.K. Riede, K. Leo, *Appl. Phys. Lett.* **93**, 103311 (2008)
13. S.K. Hau, H.-L. Yip, H. Ma, A.K.-Y. Jen, *Appl. Phys. Lett.* **93**, 233304 (2008)
14. H. Schmidt, H. Flügge, T. Winkler, T. Bülow, T. Riedl, W. Kowalsky, *Appl. Phys. Lett.* **94**, 243302 (2009)
15. M.L. Wang, Q.L. Song, H.R. Wu, B.F. Ding, X.D. Gao, X.Y. Sun, X.M. Ding, X.Y. Hou, *Org. Electro.* **8**, 445 (2007)
16. J.C. Bernède, L. Cattin, S. Morsli, F. Daou, A. Khelil, submitted
17. A. Latef, J.C. Bernède, *Phys. Stat. Sol. (a)* **124**, 243 (1991)
18. M. Morsli, C. Amory, A. Bougrine, L. Cattin, J.C. Bernède, *J. Phys. D Appl. Phys.* **40**, 7675 (2007)
19. B.P. Rand, J. Li, J. Xue, R.J. Holmes, M.E. Thompson, S.R. Forrest, *Adv. Mater.* **17**, 2714 (2005)
20. A. Godoy, L. Cattin, L. Toumil, F.R. Diaz, M.A. del Valle, G.M. Soto, B. Kouskoussa, M. Morsli, K. Benchouk, A. Khelil, J.C. Bernède, *Sol. Energy Mater. Sol. Cells* **94**, 648 (2010)